Magnesium(II) polyporphine: The first electron-conducting polymer with directly linked unsubstituted porphyrin units obtained by electrooxidation at a very low potential

Mikhail Vorotyntsev, Dmitry Konev, Charles H. Devillers, Igor Bezverkhyy, Olivier Heintz

Electrochimica Acta xxx (2010) xxx–xxx

Contents lists available at ScienceDirect

Electrochimica Acta

journal homepage: www.elsevier.com/locate/electacta

Magnesium(II) polyporphine: The first electron-conducting polymer with directly linked unsubstituted porphyrin units obtained by electrooxidation at a very low potential

Mikhail A. Vorotyntsev[a,*], Dmitry V. Konev[a,1], Charles H. Devillers[a,*], Igor Bezverkhyy[b], Olivier Heintz[b]

[a] Institut de Chimie Moléculaire de l'Université de Bourgogne, Université de Bourgogne, CNRS UMR 5260, 21078 Dijon, France
[b] Institut Carnot de Bourgogne, Université de Bourgogne, CNRS UMR 5209, 21078 Dijon, France

ARTICLE INFO

Article history:
Received 9 April 2010
Received in revised form 1 June 2010
Accepted 1 June 2010
Available online xxx

Keywords:
Electroactive materials
Electropolymerization
Magnesium porphine
Unsubstituted porphyrin
Conducting polymer
C–C coupling

ABSTRACT

Electrooxidation of magnesium(II) porphine, a totally unsubstituted porphyrin, in acetonitrile solution under potentiostatic or potentiodynamic regime leads to a polymer film at the electrode surface. Polymer deposition takes place at extremely low potential, several hundred mV less positive even compared to the deposition potential for pyrrole or EDOT (at identical monomer concentrations) in the same solvent. Film thickness can be controlled by the passed deposition charge. This material and its THF-soluble fraction have been characterized by various electrochemical methods as well as by UV–visible and IR spectroscopies, XPS, XRD and MALDI-TOF techniques. This analysis has allowed us to conclude that the polymer film is composed by chains of Mg porphine building blocks, with single bonds between the neighboring units. In the course of the potential sweep, this polymer film demonstrates a redox response resembling that of polythiophene-coated electrodes. Namely, the film is electroactive and electronically conducting in two potential ranges (p- and n-doping), which are separated by a broad interval where the film possesses a much higher resistance. The polymer may be switched between all these redox states repeatedly by the change of the potential. The film capacitance in the electroactive potential intervals is proportional to the deposition charge.

1. Introduction

Porphyrin and porphyrin-based species represent the object of intensive studies during several last decades, with thousands publications appeared each year [1]. Owing to their chemical stability and specific physical and chemical properties these materials have been proposed for various applications in catalysis and electrocatalysis, non-linear optics, luminescent devices, microelectronic elements, etc. Besides, porphyrins play an important role in numerous biomolecules.

Terminologically, the ***porphyrin family*** is based on the principal building block, ***porphine ring*** composed from 4 pyrrole groups linked in their *2,5* positions by methylene bridges. All 4 nitrogen atoms of pyrroles are oriented inside the ring and they may associate either two hydrogen atoms giving ***free-base porphine*** (Fig. 1a), or a metal cation for ***metalloporphines***, e.g. Mg^{2+} for magnesium porphine (Fig. 1b). Principally because of the easier synthetic availability, the dominant majority of studies deal with *porphyrins*, i.e. porphines with partial or full substitution at these carbon positions, by aromatic, aliphatic or more sophisticated functionalized groups.

In view of the aforementioned promising properties, porphyrins have been incorporated into numerous polymeric or oligomeric materials, to provide them with new functionalities. Towards this goal, three main approaches have been developed.

The first approach pertains to porphyrins, which are not included into the conjugation network of the polymer. These macrocycles can be linked via (conjugated or saturated) covalent bonds to a polymerizable fragment, as pyrrole, aniline or thiophene [2,3]. Another possibility to incorporate porphyrins into a solid matrix is to trap, during the polymerization process (owing to electrostatic interactions), porphyrin-bearing ionic groups such as COO^-, SO_3^-, NR_3^+ or pyridinium [2,4]. Metalloporphyrins can also be linked together by axial coordination of bridging ligands such as bipyridine and DABCO on the metal cations, thus providing so-called "shish-kebab" coordination polymers [5].

The second approach concerns copolymers or co-oligomers with alternating porphyrin and aryl, thiophene, aniline or ethynyl units inside the principal conjugated chain [6]. They have been obtained

* Corresponding authors. Tel.: +33 3 80 39 91 25; fax: +33 3 80 39 60 65.
E-mail addresses: mv@u-bourgogne.fr (M.A. Vorotyntsev), charles.devillers@u-bourgogne.fr (C.H. Devillers).
[1] Tel.: +33 3 80 39 91 25; fax: +33 3 80 39 60 65.

0013-4686/$ – see front matter © 2010 Published by Elsevier Ltd.
doi:10.1016/j.electacta.2010.06.001

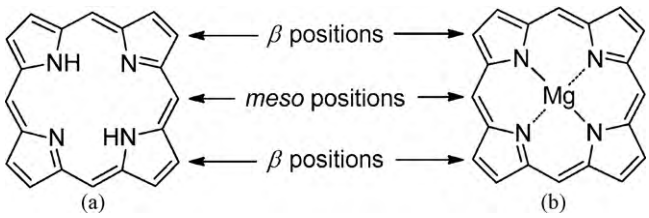

Fig. 1. Structures of (a) free-base porphine, (b) magnesium (II) porphine, MgP.

by electrochemical oxidation of the corresponding monomer [7–9] or by chemical synthesis [10,11].

The third approach consists in synthesizing solute oligoporphyrins as linear or branched chains in which the neighboring porphyrin units are directly linked in *meso* or/and *β* positions while other *meso* positions of the monomer were made non-reactive owing to protecting groups (aryl, alkyl, etc.) surrounding the ring [12–18].

To our best knowledge, no polymers (neither homopolymers nor copolymers) with ***porphine*** building blocks, i.e. ***completely unprotected*** porphyrins have been synthesized and no polymer systems with incorporated ***porphine*** moieties are known.

Assuming that a totally unsubstituted porphyrin should undergo very efficient oxidative C–C coupling between porphine units, we have very recently described the redox reactivity of magnesium porphine (MgP) [19]. It has been shown that it was possible to generate directly linked porphine oligomers in dichloromethane solution by applying a potential corresponding to the first oxidation potential of MgP. At the end of the electrolysis, a deep purple material was systematically deposited on the platinum anode. Interested by this intriguing material, we have discovered that it is possible to electropolymerize MgP on an electrode surface.

Thus, the goal of our actual study was to synthesize electroactive films of this type by means of the electrochemical oxidation of the ***magnesium(II) porphine*** monomer, MgP (Fig. 1b). The choice of the coordinated cation, Mg(II), stems from the easier synthetic access to the porphine family recently reported for MgP by Lindsey's group [20]. Moreover, among free-base and metalloporphyrins, magnesium porphyrins exhibit one of the lowest first oxidation potential [21] which is of particular interest to avoid "overoxidation" of the electrogenerated material, well-known for electroactive/conducting polymers. In addition, magnesium porphyrins are involved in photosynthetic process [22,23] and thus polymeric films of MgP may be expected to possess interesting photophysical properties.

The first results on the electropolymerization of MgP and the characterization of the new synthesized electroactive materials are presented below.

2. Experimental

MgP monomer was synthesized according to Lindsey's procedure [20]. The data (^{1}H NMR, ^{13}C NMR, UV–visible absorption, and MALDI-TOF) were consistent with those in [20].

Acetonitrile (**AN**) for polymerization and cyclic voltammetry (**CV**) studies of the film in a monomer-free solution was HPLC grade (Prolabo) with initial water content <0.02% used without further treatment. Tetrahydrofuran (THF) for partial polymer film dissolution (Acros Organics) was distilled over metallic Na + benzophenon (Merck). $TBAPF_6$ (Fluka) was dried at 80 °C for several hours prior to the use.

Electrochemical measurements (film deposition and its characterization in the monomer-free solution) were performed in AN under Ar atmosphere (after deoxygenation of solution by vacuum pumping) in three-electrode glass cell, with working electrode (WE) being Pt or glassy carbon (GC) disk or ITO-layer covered glass plate (with surface areas of about 0.01, 0.085 or 0.70 cm^2, respectively), with Pt wire as counter electrode and Ag/0.01 M $AgNO_3$ + 0.1 M $TBAPF_6$ + AN as reference electrode (RE) separated by double frit with intermediate background solution (0.1 M $TBAPF_6$ + AN).

All potentials in the paper are given *vs.* this RE. Its potential *vs.* aq. SCE is 0.32 V [24]. Formal potential of the Fc/Fc^+ couple in AN *vs.* RE is 0.10 V. More detailed information on the cell, electrode and procedures is available in reference [24]. Polymerization bath (with the same electrolyte, 0.1 M $TBAPF_6$) contained monomer solution, 0.25–1.0 mM MgP in AN. All potentiodynamic experiments (polymerization, redox response of films) were performed at the scan rate of 100 mV/s.

Homogeneity of the deposited film at the macroscopic scale was controlled by optical microscope (Nikon SMZ1000). After the deposition film was rinsed several times in AN, then transferred into background electrolyte solution in electrochemical or spectroscopic cell.

UV–visible spectra of solutions or film-coated ITO electrodes were recorded with VARIAN UV–visible spectrophotometer Cary 50 scan. For measurements of solution spectra a quartz cell with 2 mm optical path length was used. IR ATR spectra were studied with Bruker Vector 22 FT-IR spectrophotometer with MKII Golden Gate Single Reflection ATR System. XPS analysis of the monomer and films deposited on ITO was performed on a SIA100 spectrometer (Cameca Riber apparatus) using non-monochromated Al Kα X-ray source (1486.6 eV photons). X-ray powder diffractograms of films on the surface of a Pt plate were recorded in a grazing angle configuration using a position sensitive CPS 120 INEL detector with monochromated Cu Kα radiation. Mass spectra of the components of the deposited material soluble in THF were obtained on a Bruker ProFLEX III spectrometer (MALDI-TOF) using dithranol as matrix.

IR ATR and XPS spectra of the polymer material were measured for films deposited on the surface of a Pt plate. For the sake of comparison such spectra were also recorded for monomer layers obtained by repeating several times the procedure of placing a drop of the MgP + AN solution on the Pt surface, with subsequent evaporation of the solvent by drying in air. Since the literature IR spectra for MgP were registered for its microcrystalline powder (inside KBr pellet) we have also measured IR ATR spectra for our monomer in its powder state. Experimental IR transmittance spectra have been transformed into absorption ones, with subtraction of the background signal.

For extraction of soluble components of the deposited material the film-coated electrode (ITO or Pt plate) was placed into THF, then the solution was concentrated by the solvent evaporation. In the alternative procedure the polymer was deposited on the surface of a porous carbon electrode, with subsequent extraction by THF. Thus obtained solutions were used to measure their MALDI-TOF and UV–visible spectra.

3. Results and discussion

3.1. Monomer oxidation and film formation

If the potential of a bare electrode (Pt, glassy carbon, ITO) in contact with the MgP-containing electrolyte solution in AN is swept in the positive direction one can see several successive oxidation waves (Fig. 2a), the peak potential of the first wave being at about 0.4 V (Fig. 2a and b). The presentation of these data in the form of a "reduced voltammogram" (Fig 2a) where the current is divided by the monomer concentration, *c*, and by the square root of the scan rate, $v^{1/2}$, demonstrates the proportionality of the anodic current to each of these parameters and no displacement of the first

Please cite this article in press as: M.A. Vorotyntsev, et al., Magnesium(II) polyporphine: The first electron-conducting polymer with directly linked unsubstituted porphyrin units obtained by electrooxidation at a very low potential, Electrochim. Acta (2010), doi:10.1016/j.electacta.2010.06.001

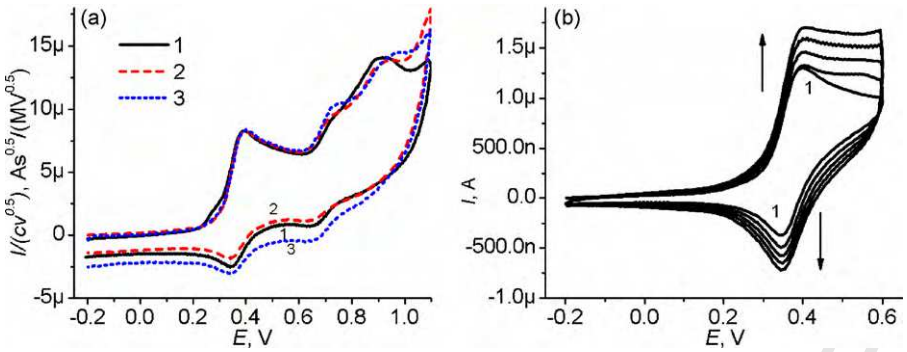

Fig. 2. (a) "Reduced" CV responses of bare Pt electrode (first scans) in MgP + 0.1 M $TBAPF_6$ + AN solutions: current, I, was divided by MgP concentration and by square root of scan rate. Various MgP concentrations or/and scan rates: 1–0.76 mM, 100 mV/s; 2–0.46 mM, 100 mV/s; 3–0.46 mM, 300 mV/s; (b) multi-cycle CV response of bare Pt electrode in 0.5 mM MgP + 0.1 M $TBAPF_6$ + AN solution. Scan rate: 100 mV/s. Anodic limit: 0.6 V. All potential values in this paper are given *vs.* Ag/0.01 M $AgNO_3$ + AN.

peak potential. The shape of these voltammograms is in conformity with observations for numerous substituted porphyrins [1] where several oxidation waves is usually observed which are related to generation of the corresponding cation radical, dication, etc.

In this paper we present results for the monomer and the deposited film only for the potential range below 0.5–0.6 V. Electrooxidation of the monomer or of the film at a higher potential results in formation of quite a different electroactive material, the properties of which will be discussed in another paper [25].

If the potential sweep is restricted to the first oxidation wave (with 0.5–0.6 V as anodic potential limit), the shape of the ***first-cycle*** at the bare electrode surface (line 1 in Fig. 2b) corresponds to a rapid electron transfer reaction with participation of ***solute*** reactant and product, rather than that within the adsorbed layer. In particular, we observe a pair of well-developed anodic and cathodic waves, with the difference between their peak potentials, $\Delta E_p = 54–56$ mV for 100–300 mV/s (for data in Fig. 2a and b), being close to the theoretical value for the E_{rev} mechanism with $n = 1$. However, the intensity of the cathodic wave is much lower than the predicted one for a pure electron transfer (the ratio of the "corrected" cathodic peak current to the anodic one is below 0.5), testifying in favor of a follow-up chemical reaction of the product of the electrochemical step, cation radical ($MgP^{\bullet+}$), with the monomer or another cation radical (EC mechanism).

This conclusion on the generation of irreversibly transformed products is confirmed by observations for subsequent cycles within the same potential interval (Fig. 2b). The intensities of both the anodic and cathodic waves increase progressively in the potential range above 0.2–0.3 V, compared to the first-cycle response, together with the change of the shape of the anodic branch. This all testifies in favor of deposition of an electroactive film, giving an additional contribution into the overall current due to the change of its redox charge.

Optical microscopy (Fig. 3) confirms the formation of a solid colored film uniformly covering the electrode surface, whose thickness grows with the number of potential scans, as it follows from the visual (intensification of the film's color) and electrochemical (see below) evidences.

Films of the same type can also be deposited in the potentiostatic regime, with the potential step from 0 V to 0.25–0.45 V (Fig. 4a). A characteristic feature of this chronoamperometric curve is the absence of the minimum of the current between the short-time decreasing branch and the stabilized region while such a minimum is usual for conventional electron-conducting polymers. The latter is generally attributed to polymer nucleation effects at the bare electrode surface [22,23]. The absence of this minimum (such behavior has already been observed, e.g. for PEDOT deposition from a microemulsion [26]) might be related to a different rate-determining step of the process within this initial period (compared to the process for most conjugated polymers), e.g. if the process is controlled by diffusion of the monomer from solution to the uniformly accessible surface or by the rate of the one-dimensional growth of the oligomer/polymer chains, without increase in the active surface area [27]. Another possible explanation of the absence of the current minimum is a different deposition mechanism where poorly soluble oligomer molecules form aggregates already inside the solution phase and then are attached to the electrode surface.

The rate of the film deposition increases with the MgP concentration (lines A and B in Fig. 4a). This process may also be accelerated by a higher deposition potential (within the interval from 0.25 V to 0.45 V), still resulting in electroactive films with similar properties, but the deposition efficiency becomes lower for higher potentials (see the next section). Sequential depositions from the same monomer solution under constant conditions demonstrate practically identical current–time curves (series of lines A and B in Fig. 4a) and redox responses of deposited films (Section 3.2), i.e. a good reproducibility of the deposition process. The polymerization rate depends also on hydrodynamic conditions. In particular, mechanical stirring of solution accelerates the film growth (lines A and C in Fig. 4a).

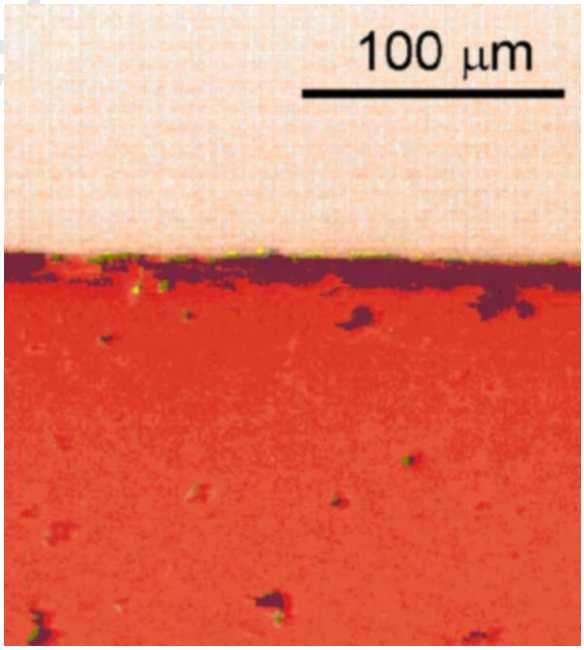

Fig. 3. Optical microscopy image of a film deposited at 0.35 V on ITO covered glass plate.

Please cite this article in press as: M.A. Vorotyntsev, et al., Magnesium(II) polyporphine: The first electron-conducting polymer with directly linked unsubstituted porphyrin units obtained by electrooxidation at a very low potential, Electrochim. Acta (2010), doi:10.1016/j.electacta.2010.06.001

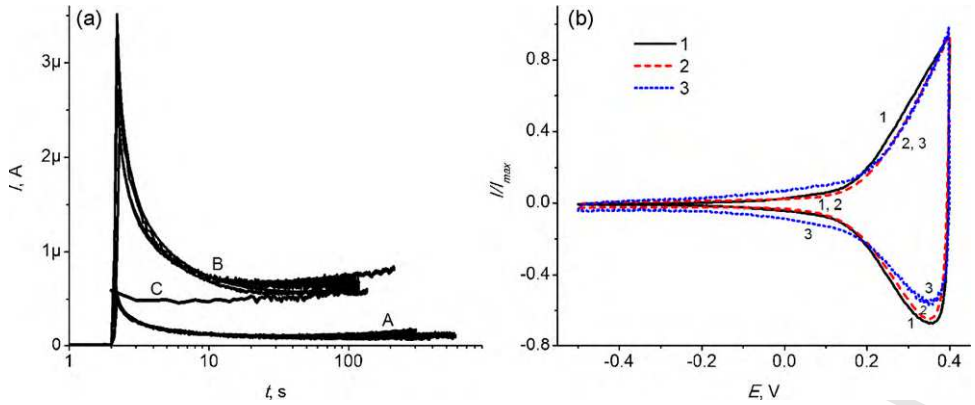

Fig. 4. (a) Potentiostatic deposition curves at $E = 0.35$ V under various conditions. Series A: 0.25 mM MgP, no stirring. Series B: 1 mM MgP, no stirring. Curve C: 0.25 mM MgP, with stirring. Curves for each series, A or B, were measured sequentially from the same monomer solution. (b) Shape of redox responses of films deposited at various conditions. Electrode material: Pt (1, 3) or ITO (2). Deposition potential: 0.35 V (1, 2) or 0.45 V (3). Monomer concentration: 0.5 mM (1, 2) or 0.25 mM (3). Deposition charge: 30 mC/cm^2 (1), 6.5 mC/cm^2 (2) or 6 mC/cm^2 (3). With stirring (1) or without agitation (2, 3). All solutions: 0.1 M $TBAPF_6$ in AN. Measured CV curves were normalized by dividing the current by its anodic maximum, I/I_{max}. Each of these responses was registered during 5 consecutive cycles (a single cycle is shown in the graph), the corresponding CV curves being practically coincident.

Parallel to the film deposition the oxidation of MgP in AN solution both in the potentiodynamic and potentiostatic regimes leads to the generation of solute products. Their analysis with the use of UV–visible absorption spectroscopy and MALDI-TOF mass spectrometry showed that they represent a mixture of the dimer, trimer and longer-chain oligomers, in which the MgP units are linked by single *meso*–*meso* bonds as it was already observed in CH_2Cl_2 [19].

3.2. Redox properties of the deposited film

The response of the film-coated electrode in monomer-free solution (Fig. 4b) in the multi-cycle experiment is perfectly stable if the cathodic limit is above −0.5 V and the anodic one does not exceed 0.4 V (treatment of the film with a higher potential leads to its irreversible oxidation, modifying it into quite a different electroactive material [25], the transformation rate being relatively low for 0.5–0.6 V while increasing rapidly for higher potentials). Variation of the deposition parameters as polymerization charge, MgP concentration, deposition potential (within the aforementioned limits), stirring conditions, etc. changes the intensity of the redox response of the film, in particular the maximum anodic current, I_{max}, while its shape, I/I_{max} *vs.* E, remains practically the same (Fig. 4b).

The redox response of the film for various scan rates is shown in Fig. 5a in the form of a "reduced voltammogram" where the current was divided by the scan rate, i.e. i/v *vs.* E, while the dependence of the maximum anodic current on the scan rate is given in Fig. 5b.

Practical coincidence of the curves in Fig. 5a and the proportionality between I_{max} and v in Fig. 5b are observed for sufficiently low scan rates (up to about 100 mV/s for the anodic branch). It implies that the film is charged (or discharged) in a uniform manner, with the instantaneous level of the charging degree being close to its equilibrium value for the potential value at that moment. A deviation from this limiting behavior takes place for higher scan rates (Fig 5a and b) due to ohmic potential drop in solution and/or slow electron-ion charge transport across the film.

The overall redox charges within this potential range (from −0.5 V to 0.4 V) for the anodic and cathodic scans are well balanced, $Q^{an}_{redox} \cong Q^{cat}_{redox}$ (Fig. 5c), and denoted below as Q_{redox}. Both redox charges diminish with increase of the scan rate (Fig. 5c), due to the above-mentioned kinetic factors. The redox charge for low scan rates characterizes its thermodynamic value for this film.

These features as well as the symmetry of the anodic and cathodic branches in Fig. 5a (especially for low scan rates) represent a proof that the film possesses sufficiently high electronic and ionic conductivities within the potential range of its electroactivity, from about 0 V to 0.4 V. This conclusion is also confirmed by the possibility to grow these electroactive films electrochemically up to a thickness well above the molecular scale since this process always requires to realize the electronic charge transport from the electrode to the ***external*** surface of the film where the new portion of monomer is oxidized (or reduced). Therefore, the deposited material must be electronically conducting at least at the polymerization potential, about 0.3–0.4 V for the system under study.

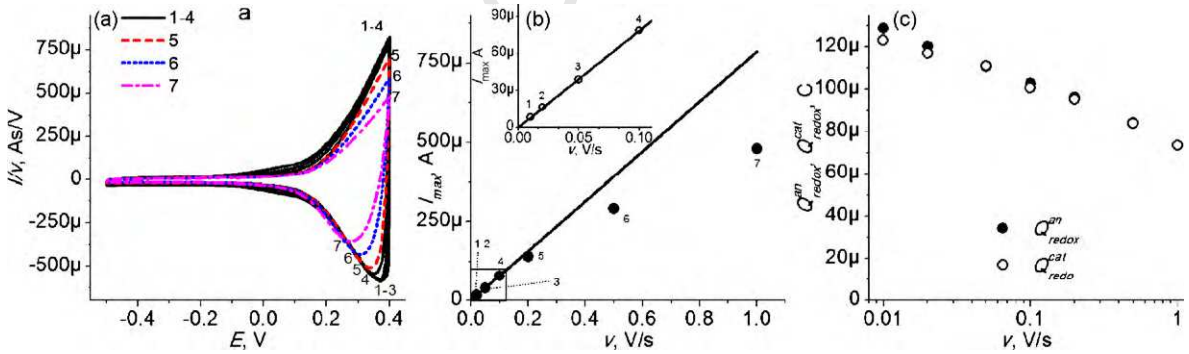

Fig. 5. Redox response of a film on ITO electrode in contact with 0.1 M $TBAPF_6$ + AN solution for various scan rates, from 10 mV/s to 1 V/s, potential range: −0.5 V to 0.4 V. (a) "Reduced" CV curves where the current, I, for each potential was divided by scan rate. (b) Maximal anodic current, I_{max}, *vs.* scan rate, v; small square indicates the area expanded in inset. Inset: I_{max} *vs.* v plot for slow scan rates. (c) Anodic (Q^{an}_{redox}) and cathodic (Q^{cat}_{redox}) redox charges electrode *vs.* scan rate. Potential interval: −0.5 V to 0.4 V.

Please cite this article in press as: M.A. Vorotyntsev, et al., Magnesium(II) polyporphine: The first electron-conducting polymer with directly linked unsubstituted porphyrin units obtained by electrooxidation at a very low potential, Electrochim. Acta (2010), doi:10.1016/j.electacta.2010.06.001

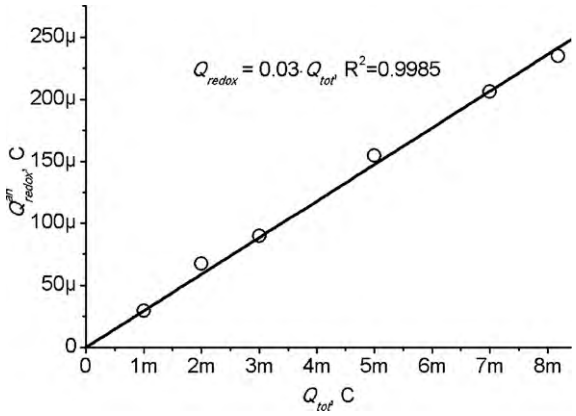

Fig. 6. Dependence of the CV redox charge of a film (deposited on ITO electrode potentiostatically at 0.35 V from 0.4 mM MgP solution, then cycled in 0.1 $TBAPF_6$ + AN solution, 100 mV/s) on the total deposition charge. Best fitting: $Q_{redox} \cong 0.03 Q_{tot}$.

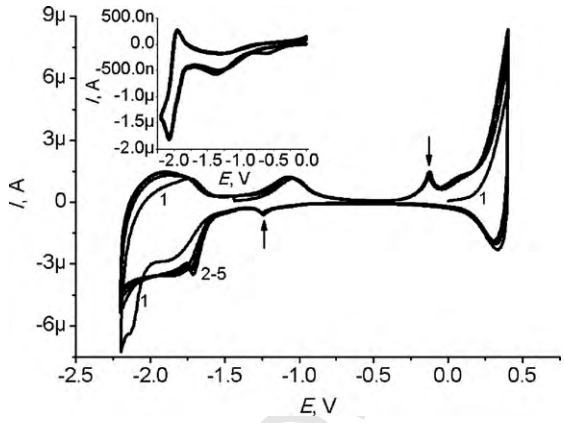

Fig. 7. CV response of film-coated Pt electrode in contact with 0.1 M $TBAPF_6$ + AN solution within a broader potential range: between −2.2 V and 0.4 V. Scan rate: 100 mV/s. Film was deposited at 0.35 V from 0.75 mM MgP solution with deposition charge of 300 μC. Vertical arrows mark spikes of the cathodic or anodic current. Inset: CV of bare Pt electrode in 0.5 mM MgP + 0.1 M $TBAPF_6$ + AN solution (with first scan in the negative potential range), 100 mV/s.

The plot of the redox charge of the film, Q_{redox}, *vs.* the total deposition charge for this film, Q_{tot}, with the other synthesis parameters being kept constant, represents a straight line passing through the origin (Fig. 6). These data imply that the deposition efficiency and the ***specific*** redox properties (per unit volume of the film) remain the same for all these films while both redox and deposition charges are proportional to the film thickness.

The value of the ratio of these charges (equal to $\eta = 0.03$ for the data in Fig. 6) may be used to evaluate the charging degree (the redox charge per monomer unit), α_{redox}, for this system at 0.4 V, with the use of Eq. (2.8) in Ref. [28]:

$$Q_{redox} = \eta Q_{tot}, \quad \eta \cong \alpha_{redox}(2 + \alpha_{redox})^{-1} f_{polym} \tag{1}$$

where f_{polym} is the fraction of the total charge during the deposition process which was spent to generate the solid deposit at the electrode surface.

The ***lower estimate*** for the charging degree, α^{min}_{redox}, corresponds to the assumption that the charge is spent completely for the film formation, $f_{polym} = 1$, which gives from the value of η and Eq. (1): $\alpha^{min}_{redox} = 2\eta(1-\eta)^{-1} \cong 0.06$. One should keep in mind that significant amounts of both (colored) oligomers in bulk solution and polymer particles deposited outside the electrode surface are observed, i.e. f_{polym} is smaller than 1 so that the charging degree, α_{redox}, is higher than this lower estimate.

The relation between the total deposition charge, Q_{tot}, divided by the surface area, A, and the film thickness, L_{film}, may be derived from Eqs. (1), (2) and (9) in Ref. [28] on the basis of the Faraday law:

$$L_{film} = \Lambda q_{tot}, \quad q_{tot} = \frac{Q_{tot}}{A} \tag{2}$$

where the proportionality coefficient, Λ, i.e. the thickness of the layer in nm deposited per 1 mC/cm^2 of the total deposition charge, is expressed via the molar volume of the monomer, v_{mon}, or the volume of the monomer molecule, v_{molec}, in the solid state:

$$\Lambda = \frac{f_{polym} f_{por}^{-1}(2 + \alpha_{redox})^{-1} v_{mon}}{F} = \frac{f_{polym} f_{por}^{-1}(2 + \alpha_{redox})^{-1} v_{molec} N_A}{F} \tag{3}$$

Here, f_{por} is the porosity factor ($f_{por} < 1$) equal to the fraction of the volume of the film occupied by the polymer molecules, N_A, Avagadro number, F, Faraday constant.

A similar relation for the film thickness and the redox charge density results from Eqs. (1) and (2):

$$L_{film} = \Lambda_{redox} q_{redox}, \quad q_{redox} = \frac{Q_{redox}}{A} \tag{4}$$

$$\Lambda_{redox} = \frac{\Lambda}{\eta} = \frac{f_{por}^{-1}(\alpha_{redox})^{-1} v_{mon}}{F} = \frac{f_{por}^{-1}(\alpha_{redox})^{-1} v_{molec} N_A}{F} \tag{5}$$

The molecular volume, v_{molec}, for our monomer, MgP, may be estimated from XRD data for the crystal composed from these species with two additional coordinated pyridine ligands [29]: $v_{molec} \approx 400$ Å^3. It results in a crude approximation for the proportionality coefficient in Eq. (2) for L_{film} in nm and q_{tot} in mC/cm^2:

$$\Lambda \approx 12 \text{ nm } (\text{mC/cm}^2)^{-1} f_{polym} f_{por}^{-1} \tag{6}$$

The value is about 5 times greater than that for polypyrrole, 2.5 nm per 1 mC/cm^2 of the deposition charge (both factors, f_{polym} and f_{por}, are usually assumed to be equal to 1 for this system) [30]. This increase of the coefficient for MgP seems to be reasonable since its molecular volume should be about 5 times greater than that of pyrrole. Nearly the same estimate for the coefficient in Eq. (2), i.e. Eq. (6), may be obtained via the first expression in Eq. (3) if the molar volume is found from the formula: $v_{mon} = M_{mon}/\rho_{mon}$ ($M_{mon} = 332$ g/mol, molecular mass of MgP), with the monomer density (in the solid state), ρ_{mon}, being about 1.3–1.5 g/cm^3, i.e. its value for polypyrrole and its alkyl derivatives for various oxidation levels [30,31].

For a known value of the total deposition charge density, q_{tot}, Eq. (2) provides the value of the film thickness if the coefficient, Λ, is available from Eq. (6). A usually used approximation consists in the assumption that the factors in this formula, f_{polym} and f_{por}, are equal to 1 or at least compensate one another, which results in a very crude estimate:

$$\Lambda \sim (10\text{–}15) \text{ nm } (\text{mC/cm}^2)^{-1} \tag{6'}$$

The extension of the potential scan for the film-coated electrode up to −2.2 V reveals relatively weak waves near −1.0 V in both directions of the scan and an extended range with anodic and cathodic currents at potentials below −1.6 V (Fig. 7). For relatively thick films, the shape of the redox response of the film near −2.0 V stabilizes after the first cycles but it varies depending on polymerization conditions (potential, agitation, monomer concentration, etc.).

Please cite this article in press as: M.A. Vorotyntsev, et al., Magnesium(II) polyporphine: The first electron-conducting polymer with directly linked unsubstituted porphyrin units obtained by electrooxidation at a very low potential, Electrochim. Acta (2010), doi:10.1016/j.electacta.2010.06.001

Similar redox activity was observed in the monomer solution at the bare electrode if the first potential scan from 0 V was made in the negative direction (inset in Fig. 7). The principal cathodic and anodic waves at bare Pt or GC electrodes (near −2.0 V) demonstrate the usual features of a reversible diffusion-controlled reaction but their shape is strongly distorted by adsorption waves and redox transformations in the adsorbed state. Thus, the reduction–oxidation transformation of solute monomer (to its anion radical and back) takes place both on (bare) Pt and GC in the same potential range as the redox activity of the deposited film.

This coincidence represents the first evidence in favor of the conclusion that the porphine unit retains its structure inside the film. A much broader shape of the redox response of the units inside the film may be attributed to electron delocalization between neighboring units (see below), combined with usual heterogeneity effects in the solid polymer phase.

A high intensity of the current in the potential ranges of the film electroactivity, above 0 V and below −1.4 V, related obviously to the change of the oxidation/charging level of this material provides an evidence that this medium becomes ***electronically conducting*** for these potential intervals since for this process the electronic charge has to be transported between the electrode and the recharging units of the material far away from the electrode surface. Another argument in favor of the conducting type of this material in the potential range around 0.3–0.6 V follows from Fig. 2b: the intensity of the monomer oxidation wave and the reduction wave of the generated cation radical do not diminish in the course of cycling. These reactions of solute species take place despite the growth of the deposited film separating the electrode surface and the monomer oxidation places at the external surface of the deposit. A more quantitative characterization of the film conductivity is given below.

These redox properties resemble closely those of conventional conjugated/conducting polymers (e.g. polythiophene), with their ranges of electroactivity at sufficiently high positive ("p-doping") and negative ("n-doping") potentials, separated by the interval without electroactivity with a very low redox response. The limits of this insulating range, from −0.2 V to −1.2 V, manifest themselves by characteristic spikes of the CV current (marked by vertical arrows in Fig. 7) originating from rapid discharge of charge carriers trapped inside the film, owing to the onset of electronic conductivity. One should note that the lower limit of this range would be markedly more negative (about −1.5 V) if it is determined by the rise of the redox response of the film, see also resistance data in the next section.

3.3. *Reactions of solute species and film resistance*

We have already indicated above that the possibility to realize the film growth electrochemically and the quasi-equilibrium redox charging of such films in a background solution at low scan rates represent a direct proof of a sufficiently high electronic conductivity of their material. Additional information on the film conductivity is provided by redox reactions of solute species at the film-coated electrode. Fig. 8 shows the result of such tests for two solute species, ferrocene (Fc) and titanocene dichloride ($TcCl_2$).

Comparison of the CV responses of the film-coated electrode in solutions with and without Fc (lines 2 and 1 in Fig. 8, respectively) reveals that the reversible pair of anodic and cathodic peaks around 0.1 V (equal to the formal potential of the Fc/Fc^+ couple) is added to the redox response of the film itself. On the contrary, the further addition of $TcCl_2$ into this solution (line 3 in Fig. 8) does not result in a cathodic wave at about −1.0 V, as it occurs at the bare Pt electrode. The corresponding $TcCl_2$ reduction wave is displaced by about 350 mV in the negative direction.

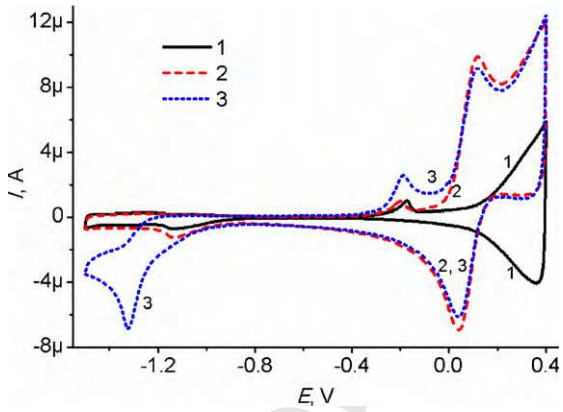

Fig. 8. CV responses (5th cycle in each series, 100 mV/s) of the film-coated Pt electrode in contact with background (0.1 M $TBAPF_6$ + AN) solution (line 1) or with solution of 2 mM Fc (line 2) or 2 mM Fc + 2 mM $TcCl_2$ (line 3). Film was deposited potentiostatically at 0.35 V from 0.5 mM MgP solution, total deposition charge 38 mC/cm^2.

The absence of the $TcCl_2$ reduction wave near −1.0 V proves directly the absence of a significant area of the Pt substrate which is not covered by the film as well as a sufficiently high electronic resistance of the film at this potential. The appearance of this wave at a more negative potential is usually considered as an implication that the electronic conductivity of the film begins to increase again at approaching the electroactivity range within the range of sufficiently negative potentials (see however the discussion below).

Then, the observation of a ***reversible*** Fc wave (despite of the complete coverage of the electrode surface by the film) means definitely a sufficiently high electronic conductivity of the film around 0.1 V. All these conductivity features correlate well with the intensity of the redox response of the film in the corresponding potential intervals.

Quantitative information of the electronic conductivity of the film is provided by potential step experiments where the extrapolation of the chronoamperometric curves to the zero-time limit allows one to determine the total high-frequency resistance which is approximately equal for our system to the sum of the solution resistance, R_s, and the high-frequency electronic resistance of the film, R_f.

The data for this sum, $R_s + R_f$, for a set of the electrode potentials are shown in Fig. 9a. They demonstrate that the total resistance in both ranges of the film electroactivity, above 0.2 V and below −1.6 V, is close to the solution resistance, about 480 Ω (this constant value is shown by horizontal line in Fig. 9a). In particular, for $E > 0.3$ V and $E < -1.9$ V the film resistance becomes so small compared to this value that we can get only its upper estimate: $R_f \ll 10\ \Omega$. On the contrary, a drastic increase of the film resistance takes place in the potential interval between these electroactivity ranges, with a maximum in the central part of this interval. The shape of this resistance–potential plot and the level of the resistance inside the insulating range depend both on the film thickness (the thicker is the film, the higher is this level) and the conditions of its deposition.

Data in Fig. 9a mean a more negative value for the lower limit for the insulating range, about −1.6 V, and correspondingly its broader extension, about 1.4 V, compared to the values based on current spikes (Fig. 7) or the wave of the $TcCl_2$ reduction (Fig. 8). The observation of significant currents for the latter cases, despite the insulating character of the material at those potentials, may be related to a relatively small thickness of the film, i.e. not very high resistance so that the overpotential, e.g. 350 mV for the $TcCl_2$ reaction is sufficient to ensure the passage of a microampere-level

Please cite this article in press as: M.A. Vorotyntsev, et al., Magnesium(II) polyporphine: The first electron-conducting polymer with directly linked unsubstituted porphyrin units obtained by electrooxidation at a very low potential, Electrochim. Acta (2010), doi:10.1016/j.electacta.2010.06.001

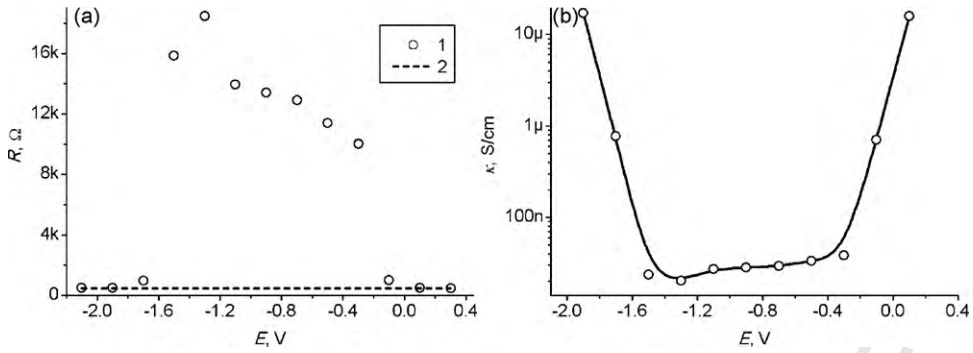

Fig. 9. Dependence of (a) the total resistance, $R_s + R_f$, and (b) the film conductivity on the electrode potential. Pt disk electrode coated with deposited film whose thickness, about 300–450 nm, was estimated with the use of Eqs. (2) and (6′) for the total deposition charge of 30 mC/cm². Data in (a) were obtained by means of a set of cathodic potential steps with constant 0.1 V amplitude in the potential interval from 0.3 V to −2.2 V. Dashed line in (a) corresponds to the high-frequency resistance for the bare electrode without film, $R_s = 480\ \Omega$.

current across the layer with the resistance of the order of tens of kΩ.

With the use of the electrode surface area and of Eqs. (2) and (6′) to estimate crudely the film thickness, one can recalculate the data in Fig. 9a to determine the dependence of the specific electronic conductivity of the film, κ_f, on the potential (Fig. 9b). Inside the non-electroactivity potential interval the conductivity drops up to a very low level (tens of nS/cm). Near the onset of the p- or n-electroactivity it demonstrates a drastic rise, about three orders of magnitude by 0.2 V for the film oxidation, or −1.8 V for its reduction. This increase continues obviously for higher charging levels but, analogously to the data for the resistance, this method only allows one to give a lower estimate of the conductivity in these potential ranges: $\kappa_f \gg 0.02$ mS/cm.

It is worth to note that the minimal conductivity for such well-known conducting polymers as *N*-alkyl substituted derivatives of polypyrrole is about 1 μS/cm while the maximal one is only of the order of 1 mS/cm. In this context the new material corresponds well to the term "conducting polymer" within its electroactivity ranges while the range of variation of its conductivity is expectedly much broader.

3.4. IR spectroscopy

Complete analysis of the vibrational structure and the IR spectra of individual porphyrin molecules, in particular those of MgP has been carried out with the use of quantum-chemical methods [32]. On the contrary, such calculation has never been made for extended porphyrin structures, even for their dimers, i.e. one cannot rely upon theoretical results in interpretation of the IR data for our (expectedly polymer) material.

Therefore, our analysis of the IR spectrum of the film will be based on its comparison with the experimental data for monomeric porphines. As the primary step the measured ATR IR spectrum of our monomer (MgP) powder (Fig. 10b) was compared with the literature one for the MgP powder inside KBr pellet [32] (Fig. 10a) as well as with theoretical values for IR-active vibrational frequencies for this molecule [32]. A very good agreement between the spectra and between the values of the maximums enables us to conclude both on a high purity of our monomer and on the reliable measurements of the spectra. The further comparison of the IR spectra for our monomer in the forms of powder (Fig. 10b) or of a layer at the Pt surface (Fig. 10c) reveals differences in some secondary features (in particular, the noise below 650 cm^{-1}) but all principal bands are practically identical in both spectra.

Then, the IR spectra of the monomer layer (Fig. 10c) and of the polymer film (Fig. 10d) reveal a very close similarity, both in positions of the principal lines and in their relative intensities. It means that the whole vibrational structure of the porphine is retained inside the deposited material, i.e. that ***the film is composed from intact porphine building blocks***. Moreover, this identity of vibrational structures of the material and the monomer excludes the formation of ***multiple*** bonds between the units since it would affect strongly the vibrational properties of the atoms included into such bonds.

The next question is on whether the Mg cations are retained inside porphine units inside the material in the course of the polymerization procedure. To answer this question the IR spectrum of the free-base porphine, H_2P (Fig. 1a), was also measured (Fig. 10e) which was in a good agreement with literature data [33]. Comparison of the spectra for MgP and H_2P porphines [33–36] provided

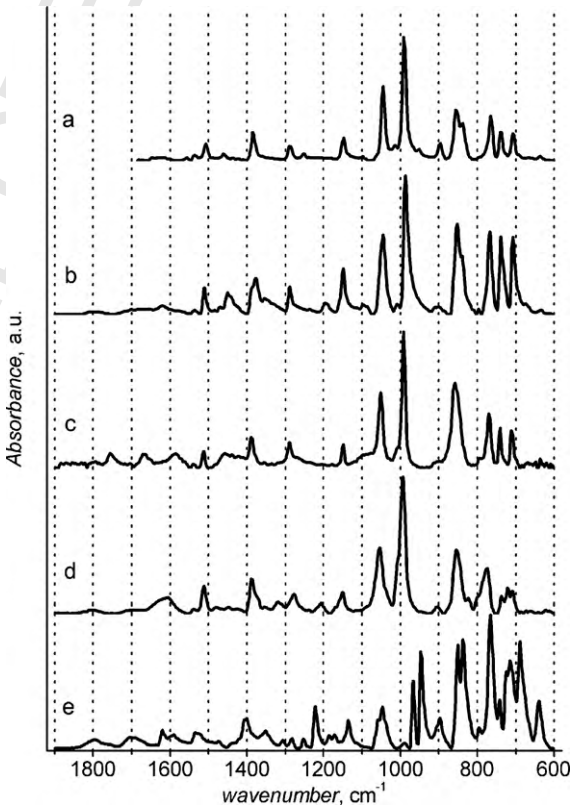

Fig. 10. IR absorption spectra (only the range between 600 and 1900 cm^{-1} is shown): (a) from transmission spectra of monomer (MgP) powder inside KBr pellet (data of [32] after subtraction of background absorption); (b–e) our samples, ATR mode: (b) monomer (MgP) powder; (c) monomer (MgP) layer on Pt plate; (d) polymer film deposited on Pt plate; (e) powder of free-base (H_2P) porphine.

Please cite this article in press as: M.A. Vorotyntsev, et al., Magnesium(II) polyporphine: The first electron-conducting polymer with directly linked unsubstituted porphyrin units obtained by electrooxidation at a very low potential, Electrochim. Acta (2010), doi:10.1016/j.electacta.2010.06.001

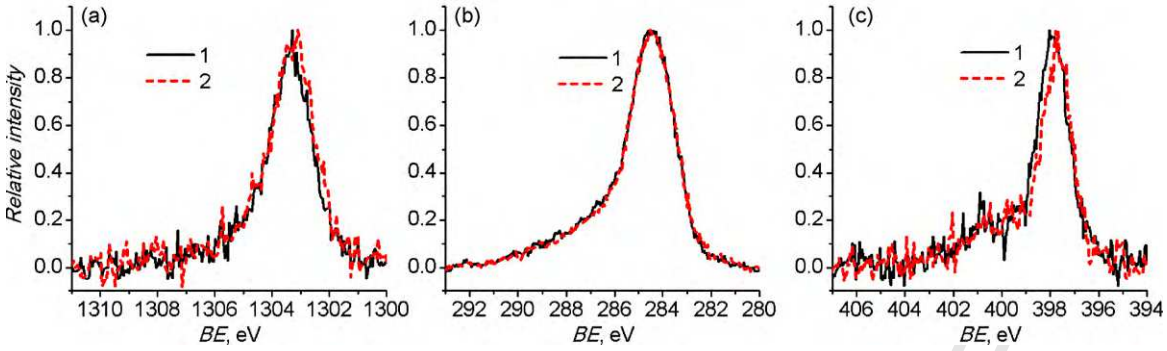

Fig. 11. XPS spectra for the MgP monomer (line 1) and for deposited film (line 2): (a) Mg 1s, (b) C 1s, (c) N 1s.

several wave length intervals with a qualitatively different behavior: (1) absorption bands at about 680 and 3320 cm^{-1} (not shown in Fig. 10) related to vibrations of nitrogen-bonded H atoms inside the cavity, only present for H_2P [33,34], (2) very intensive bands at about 990 and 1050 cm^{-1} in the spectrum of MgP while less intensive bands are visible for H_2P at about 950 and 965 cm^{-1}. Analysis of the spectrum of the film (Fig. 10d) revealed its perfect agreement with the spectrum for Mg containing species but no features of the free-base one. Therefore, one may conclude that ***Mg cations are not lost*** during the film formation or the electrode cycling in background solution.

Thus, the IR data for the synthesized material testify in favor of its structure as polymer chains with single bonds between magnesium porphine units so that it may be called "polyporphine" or more accurately "poly(magnesium(II)-porphine)" (**pMgP**).

3.5. XPS

To characterize both the ratio of elements inside the deposited material and the oxidation states of the elements in it, XPS spectra were measured in parallel for a solid layer of the monomer, MgP, deposited on Pt plate from AN solution and for electropolymerized polyporphine films on ITO electrode surface. Calibration factors for the recalculation of the integral intensity of the peak for each element in the experimental spectrum into its atomic content were determined from the data for the monomer, in particular to get the proper ratio, 1:4, of the atomic contents of Mg and N. Then, these factors were used for the treatment of the XPS spectra for polyporphine films. The average ratio of the atomic contents of Mg and N for polyporphine films, 1.01:4, turned out to be identical to that for the monomer, within the experimental precision (±5%).

This conservation of the Mg-to-N ratio in the course of the polymerization represents an important indication on the structure of the obtained material. The electron-conducting property of the polymer at the potential of its deposition (see above) implies the electronic conjugation between the neighboring monomer units. The latter means that the formation of the chemical bonds between these units must be accompanied by ***release of protons*** (two protons per each bond), i.e. by increase of the local acidity. Therefore, one cannot exclude ***a priori*** that these protons may replace magnesium cations inside porphine units, both in dissolved monomer and inside the polymer. The above XPS data demonstrate that the polymerization in the chosen mild conditions (at a very low oxidation potential, with a weak current intensity) liberated protons leave into the bulk solution, practically without demetallation of porphine units inside the polymer.

Comparative analysis of the data for the polymer and for the monomer was also applied to the XPS spectra of each element, Mg, C and N, to characterize their oxidation states.

The shapes and positions of the XPS spectra of Mg 1s (Fig. 11a, maximum at 1303.2 eV) and C 1s (Fig. 11b, maximum at 284.5 eV) are practically identical for monomer and polymer. This is also valid for the N 1s spectrum (Fig. 11c): its shape is practically the same for the monomer and for polyporphine film, being composed from the principal peak at 307.7 eV and a shoulder shifted to higher energies by about 1.9 eV, their relative weights being about 80%:20%.

These observations confirm the conclusion based on the above IR analysis that the deposited material represents a polymer composed from intact porphine units, with Mg cations retained inside them. The shapes of all elements correspond well to literature XPS data for porphyrins, in particular the above shape of the N 1s spectrum (including the position and the relative intensity of the shoulder) reproduces nicely those that for monomeric MgTPP [37]. The conclusion on the porphine ring conservation is also in conformity with the absence of carbon–oxygen (286–289 eV [38–40]) or nitrogen–oxygen (403–407 eV [41]) bonds in C and N spectra for these films.

The XPS spectra of the polyporphine films do not show significant bands of P or F which would be related to counter-ions, PF_6^-, from background electrolyte incorporated into the deposited material to compensate the positive charge of the polymer matrix. On the contrary, the presence of these elements was visible in control XPS experiments with polymer films of the polypyrrole family. We do not believe that the absence of the P and F signals for pMgP deposits is due to release of anions from the film due to its discharge during the electrode extraction from the solution (for the further XPS studies) where the control of the oxidation level by the electrode potential is inevitably lost, since the OCP measurement in solution does not show a rapid potential evolution. More probably, the difference observed for pMgP and substituted polypyrrole films should be attributed to a much higher content of these anions in the latter materials: the typical charging degree for these polymers is about 0.25–0.3 of the (positive) electron charge per monomer unit, i.e. 0.06–0.075 of anion per carbon atom of the pyrrole ring. A crude estimate of the charging degree, α_{redox}, e.g. for the polyporphine film used for XPS measurements was about 0.06 of the electron charge per MgP unit, i.e. about 0.003 of PF_6^- anion per carbon atom of the MgP unit. It means that the relative intensity of the P and F bands in XPS spectrum for the polyporphine system is expectedly about 20–25 times less intensive than that for polypyrrole films, too weak for detection due to the noise of the XPS signal.

3.6. UV–visible spectroscopy

According to the exciton model [42], the direction of the broadening in the spectrum of a complex formed by several identical units, compared to the monomer bands (to higher or lower energies), should depend on the geometrical configuration of this

Please cite this article in press as: M.A. Vorotyntsev, et al., Magnesium(II) polyporphine: The first electron-conducting polymer with directly linked unsubstituted porphyrin units obtained by electrooxidation at a very low potential, Electrochim. Acta (2010), doi:10.1016/j.electacta.2010.06.001

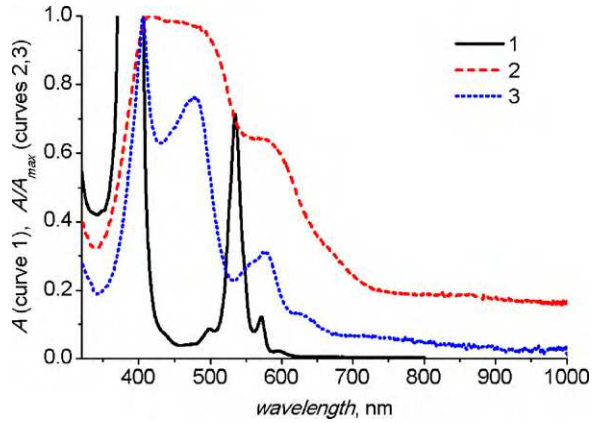

Fig. 12. UV–visible spectra: (1) monomer, MgP, in AN solution; (2) film deposited on ITO electrode (in its insulating state); (3) components of the film extracted by THF (spectra 2 and 3 are normalized, A/A_{max}, with the use of the maximal absorption of the spectrum.

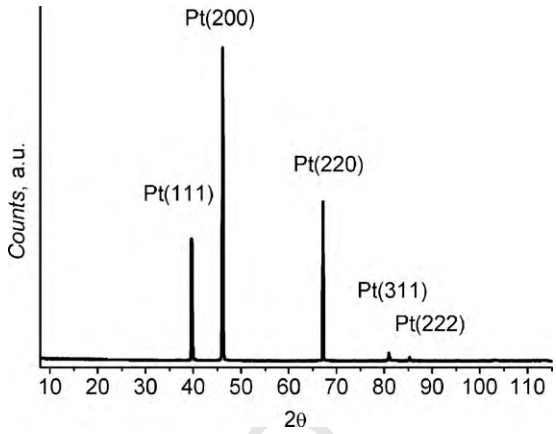

Fig. 13. XRD spectra of film deposited on Pt substrate.

complex. A blue shift may be expected, e.g. for aggregates with monomer units displaced in the direction normal to the monomer planes. On the contrary, a downward tendency for the excitation energy should be characteristic, e.g. for a linear chain of covalently linked units with the dipole moment in the excited state oriented along the inter-unit bond.

Comparison of the UV–visible spectra for the monomer (in AN solution) and for polymer film in its discharged state (lines 1 and 2 in Fig. 12, respectively) demonstrates a strong broadening of both Soret and Q-bands of the monomer after polymerization, which are transformed into plateau-type ranges, typical to spectra for polymeric materials. The downward tendency for the transitional energy allows one to exclude that our material is formed by the π-stacking of porphine units while this feature matches well the expected polymeric structure with covalent bonds between neighboring porphine units.

The observed plateau character of both former Soret and Q-bands in the spectrum of the material may be attributed to a great dispersion of the transitional energies due to variation of the dipole–dipole interaction energy because of various distances between the interacting units and various angles between their planes. The noticeable absorption in the range above 700 nm is probably related to the light scattering by supramolecular aggregates on the surface of the film or/and to residual delocalized electronic species trapped inside the film.

3.7. XRD

XRD spectrum for polyporphine film is shown in Fig. 13. All recorded peaks correspond to the values for the Pt substrate (JCPDF 01-087-0636). It means that polyporphine polymer do not possess a pronounced crystalline structure.

3.8. Soluble fraction of the film: MALDI-TOF mass spectrometry

For the further characterization of the deposited material, relatively thick films on the large-area electrodes were treated by THF, with characterization of extracted soluble components of the film. Fig. 14a shows a representative example of the MALDI-TOF spectrum for a solution obtained via the first procedure of solution preparation, in which one can see a series of isotopic patterns, each of them corresponding to the mass (for various isotopic compositions) of an oligomer (linear or zigzag type, without closed loops in its chain) composed from MgP units with a single bond between them. The second extraction procedure provides solutions of higher concentrations, i.e. a more intensive MALDI-TOF spectrum (Fig. 14b). The set of principal isotopic patterns corresponds again to expected oligomers (Table 1). In particular, the minimal mass within each isotopic pattern matches well the formula: $M_n = n(M_m - 2M_H) + 2M_H$, M_m and M_H being (minimal) masses of MgP and proton, respectively, with the values of n from 3 to 8 (Fig. 14b). The distribution of intensities within each isotope pattern is also in agreement with theoretical predictions for the corresponding oligomer with single bonds (Fig. 14c).

Hypothetically, two neighboring porphine units in a chain could form more than one (two or even three) single bond between their peripheral carbon atoms (double or triple bonds cannot be formed without a chemical change of the porphine structure), as e.g. in linear oligomers composed from porphyrin blocks by three bonds of *meso*–*meso* and two *β*–*β* types [17]. However, the oligomer with such multiple bonds would have a ***different mass***, compared to its singly bonded analog, since each extra bond means the removal of two protons. Therefore, both the "minimal mass" and the isotopic pattern as a whole for such oligomer would demonstrate a clearly visible shift to lower masses ($-2M_H$ units per supplementary bond) compared to our experimental data.

Besides the peaks related to these fully metallated oligomers one can also note "satellites" with lower masses (Fig. 14a and b) corresponding to the loss of one (or several) Mg cation from these oligomers. Their relative intensities (compared to that for the fully metallated oligomer) are higher for the second preparation procedure (Fig. 14b) since the transport of the protons generated during the polymerization on the surface of ***porous*** carbon to the bulk solution is hindered. As a result, the local acidity increases resulting in a greater loss of Mg cations from some monomer units in the film.

One should not consider the fraction of demetallated oligomers in MALDI-TOF spectrum as identical to such fraction in the initial sample analyzed by this technique. Partial demetallation of porphine units takes also place in the course of the sample ionization. It follows from our observation of an analogous satellite peak (corresponding to the free-base monomer, H_2P) in the MALDI-TOF spectrum of pure MgP monomer while the NMR spectrum of this substance shows only the metallated porphine.

Analogously, one cannot identify the distribution of intensities in spectra of Fig. 14a and b as a function of the oligomer length with that for oligomer fractions inside the deposited material since the former is also affected by the difference in their solubility and in their ionization ability.

The absence or a weak intensity of the peak for the dimer, $(MgP)_2$, in our MALDI-TOF spectra originates probably from its relatively high solubility in AN (compared to that for longer-chain oligomers) so that it is not accumulated inside the film in the course of its deposition.

Please cite this article in press as: M.A. Vorotyntsev, et al., Magnesium(II) polyporphine: The first electron-conducting polymer with directly linked unsubstituted porphyrin units obtained by electrooxidation at a very low potential, Electrochim. Acta (2010), doi:10.1016/j.electacta.2010.06.001

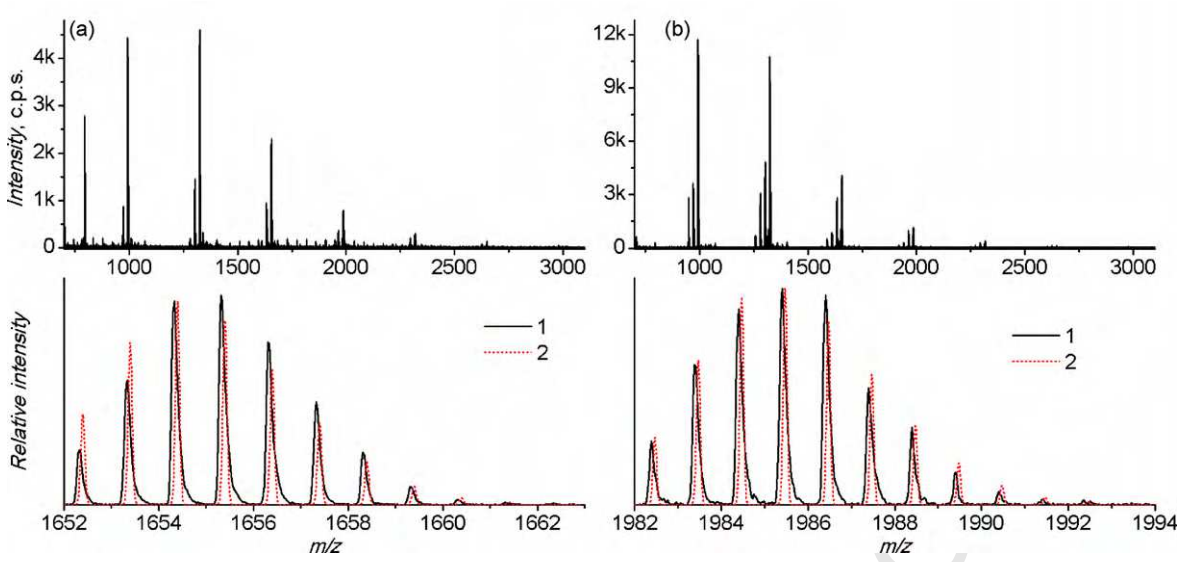

Fig. 14. MALDI-TOF mass spectra of solution prepared according to (a) first or (b) second extraction procedure. Comparison of experimental isotopic patterns (solid lines) for $n = 5$ (c) and $n = 6$ (d) with theoretical predictions (dot lines) for the corresponding oligomers composed from MgP units with single bonds between them.

3.9. Soluble fraction of the film: UV–visible absorption spectroscopy

The THF-soluble fraction of the deposited material has also been characterized by the electronic spectrum of this solution measured after its concentrating (Fig. 12, line 3). It demonstrates an obvious qualitative resemblance with the spectrum of the film (line 2 in Fig. 12), in particular broadening of both Soret and Q-bands towards lower energies. However, the plateau regions observed for the film are replaced a wider band for the Q region or a split one for the Soret range.

The splitting of the Soret band into two subbands (of equal intensities) has been observed for linear-chain ***zinc porphyrin*** oligomers in the solute state [12], the higher energy one being located near the initial Soret wave length while the shift of another subband to lower energies increases with the chain length. In this context the shape of line 3 in Fig. 12 may be interpreted as a superposition of the spectra for analogous ***magnesium porphine*** oligomers (whose presence has been proven by mass-spectrometry of this solution, see above), with the principal contribution of oligomers with 3–4 units. In particular, it explains the presence of a higher intensity peak near the position of the Soret band for the monomer (line 1 in Fig. 12) and of a broader but lower intensity subband with maximum at 480 nm.

The aforementioned differences in the shapes of the spectra for the film and its extracted fraction (lines 2 and 3 in Fig. 12, respectively) should be a consequence of several factors: (1) the insoluble fraction of the film should expectedly correspond to longer chain lengths; (2) the presence of a broader range of the chain lengths in the deposited film, compared to its soluble components; (3) the insolubility of certain components of the film may also be due to side cross-linking bridges between the chains, which affect the spectral properties; (4) mutual orientations of neighboring porphine units with respect to the bond between them should be quite different for the same oligomer molecule in the solute state (where the units tend to be oriented perpendicularly to the bond [12], due to the van der Waals repulsion between them) and inside the solid matrix (where the electronic exchange between units acts in the direction towards a more planar configuration). According to the exciton theory [42] the change of the molecular geometry and consequently the mutual orientation of transitional dipoles leads inevitably to a different shape of the oligomer spectrum; (5) at last, the spectra in the solid state are smeared out due to heterogeneity of the polymer matrix and intermolecular interactions.

3.10. Molecular structure

The IR and XPS data for the film show that both porphine unit and Mg cation are retained inside the deposited material. As for inter-unit linkage, the striking resemblance of the IR spectra for the monomer and the deposited material provides a strong argument in favor of a single bond between neighboring porphine units. The latter conclusion matches perfectly with the observation of transitions between the insulating and electron-conducting states upon variation of the electrode potential. The electronic conduc-

Table 1
Experimental data for MALDI-TOF spectra of THF extracted solutions and theoretical predictions for "minimal masses" and masses of peaks with maximal intensities for a series of linear singly linked Mg porphine oligomers.

n	Mass of the peak with the lowest mass within isotopic pattern		Mass of the peak with maximal intensity within isotopic pattern	
	Theoretical predictions	Experimental values	Theoretical predictions	Experimental values
1	332.09	–	332.09	–
2	662.17	661.92	662.17	663.20
3	992.24	992.08	993.24	993.08
4	1322.32	1322.22	1324.32	1324.23
5	1652.39	1652.32	1654.40	1655.32
6	1982.47	1982.38	1985.47	1985.41
7	2312.54	2312.46	2315.55	2316.45
8	2642.62	2642.54	2646.62	2645.55
9	2972.70	2972.57	2976.70	2976.57

Please cite this article in press as: M.A. Vorotyntsev, et al., Magnesium(II) polyporphine: The first electron-conducting polymer with directly linked unsubstituted porphyrin units obtained by electrooxidation at a very low potential, Electrochim. Acta (2010), doi:10.1016/j.electacta.2010.06.001

tivity requires a sufficiently good overlap between π-electrons of neighboring units so that the dihedral angle between them should be relatively small in this state. The transition to the insulating state implies that electrons become localized within their own unit so that the dihedral angles should increase to diminish the van der Waals repulsion, within the limits allowed by the surrounding solid matrix, thus breaking the electronic exchange. Such rotation of porphine building blocks around the inter-unit axis (even for a relatively small angle) would be impossible if a pair of neighboring units were linked by more than one bond. Moreover, such reorientation of a porphine unit inside a solid matrix would be hardly possible for two-dimensional, cyclic or zigzag structures of oligomer/polymer chains since the rotation of a porphine unit would then require a strong displacement of connected units. This reasoning leads to the conclusion on the ***linear*** polymer/oligomer structure of the deposited material.

Electronic distribution in the valent A_{2u} orbital of Mg and Zn porphyrins [43,44] results in reactions at *meso* positions [45]. In conformity with this general tendency the porphyrin with blocked *meso* positions, MgTPP, does not polymerize, a stable cation radical being formed at the potential of the first oxidation wave [46]. The same behavior was observed for a porphyrin with free *meso* positions, MgOEP [46–48], this time due to steric hindrance arising from ethyl substituents in β positions. On the contrary, mild chemical [12] or electrochemical [44,49] oxidation of Mg and Zn porphyrins with protected *5,15 meso* positions (but without substitutions in β positions) leads to corresponding linear oligomers with *meso–meso* linkage between units. Similarly, electrochemical oxidation of our unsubstituted porphyrin, MgP, results (besides the deposited polymer film) in solute linear *meso–meso* bonded oligomers [19]. Since our deposited material represent the product of a further transformation of these soluble oligomers while the above analysis testifies in favor of its structure as linear chains of MgP units one may conclude that these porphines are linked by *meso–meso* bonds.

This conclusion is in conformity with MALDI-TOF spectra of its THF-soluble fraction (Fig. 14), which correspond to various oligomers with this structure while the UV–visible spectrum of this solution (line 3 in Fig. 12) allows us to extend this result also to the insoluble fraction of the film.

The absence of any substituent in MgP, combined with other data for this system, assures that the film is formed by direct links between these monomer units. In this context the possibility to get such polyporphine chains by polymerization of MgP is due to a fortunate combination of its Mg-coordinated and substituent-free characters.

4. Conclusion

The synthesized intriguing material, "poly(magnesium(II)-porphine)" (pMgP), belongs to electroactive polymers, possessing characteristic electronically conducting states, with mobile holes ("polarons", "bipolarons") at high oxidation levels and mobile "electrons" for a strongly reduced state, separated by the non-electroactivity range in which the material is electronically non-conducting. This behavior is related expectedly to the transition between a molecular organization with small dihedral angles between porphine units for the electronically conducting state and the structure with twisted orientations of neighboring monomer units for the insulating state. On the basis of a combination of various experimental data for this material (electrochemistry, IR, XPS and UV–visible spectroscopy, MALDI-TOF mass spectrometry) we arrived to the conclusion that these polyporphine films are composed from linear molecular chains with *meso–meso* linkage between neighboring porphine units.

To our best knowledge, it is the very first example of a polymeric structure formed only by unsubstituted porphyrin units.

Owing to their very interesting photophysical (absorption within a broad UV-Vis spectral range) and electronic (very low oxidation potential, conductivity in two potential ranges) properties, one can expect that these totally new electroactive materials will find applications, e.g. in molecular electronics, non-linear optics, photovoltaics, energy sources, corrosion protection.

Acknowledgment

The authors are thankful J.M. Barbes, Yu.G. Gorbunova and P.D. Harvey for stimulating discussions. We are deeply grateful to J. Cox, Z. Galus, J. Heinze, V.M. Mirsky, R. Seeber, O.A. Semenikhin, M. Skompska and V. Tsakova for the thorough analysis of the primary version of the manuscript and the valuable comments on its improvement. The financial support of CNRS, Conseil Régional de Bourgogne, Université de Bourgogne and the Russian Foundation for Basic Research (project no. 09-03-01172a) is acknowledged.

References

[1] K.M. Kadish, K.M. Smith, R. Guilard, in: K.M. Kadish, K.M. Smith, R. Guilard (Eds.), The Porphyrin Handbook, vols. 1–20, Academic Press, 2000.
[2] F. Bedioui, J. Devynck, C. Bied-Charreton, Acc. Chem. Res. 28 (1995) 30.
[3] J.A.A.W. Elemans, R.v. Hameren, R.J.M. Nolte, A.E. Rowan, Adv. Mater. 18 (2006) 1251.
[4] M.A. Vorotyntsev, S.V. Vasilyeva, Adv. Colloid Interface Sci. 139 (2008) 99.
[5] J.-H. Chou, M.E. Kosal, H.S. Nalwa, N.A. Rakow, K.S. Suslick, Applications of porphyrins and metalloporphyrins to materials chemistry, in: K.M. Kadish, K.M. Smith, R. Guilard (Eds.), The Porphyrin Handbook, vol. 6, Academic Press, 2000, pp. 43–131, (Chapter 41).
[6] R.E. Martin, F. Diederich, Angew. Chem. Int. Ed. 38 (1999) 1350.
[7] P.A. Liddell, M. Gervaldo, J.W. Bridgewater, A.E. Keirstead, S. Lin, T.A. Moore, A.L. Moore, D. Gust, Chem. Mater. 20 (2008) 135.
[8] J. Rault-Berthelot, C. Paul-Rothab, C. Poriel, S. Juillard, S. Ballut, S. Drouet, G. Simonneaux, J. Electroanal. Chem. 623 (2008) 204.
[9] C.O. Paul-Roth, J. Letessier, S. Juillard, G. Simonneaux, T. Roisnel, J. Rault-Berthelot, J. Mol. Struct. 872 (2008) 105.
[10] H.L. Anderson, Chem. Commun. (1999) 2323.
[11] P.D. Harvey, Recent advances in free and metallated porphyrin assemblies and arrays; a photophysical behavior and energy transfer perspective, in: K.M. Kadish, K.M. Smith, R. Guilard (Eds.), The Porphyrin Handbook, vol. 18, Academic Press, 2003, pp. 63–250, (Chapter 113).
[12] A. Osuka, H. Shimidzu, Angew. Chem. Int. Ed. Engl. 36 (1997) 135.
[13] N. Yoshida, N. Aratani, A. Osuka, Chem. Commun. (2000) 197.
[14] A. Tsuda, H. Furuta, A. Osuka, Angew. Chem. Int. Ed. 39 (2000) 2549.
[15] N. Aratani, A. Osuka, Chem. Rec. 3 (2003) 255.
[16] A. Tsuda, Y. Nakamura, A. Osuka, Chem. Commun. (2003) 1096.
[17] A. Tsuda, A. Osuka, Science 293 (2001) 79.
[18] L.-M. Jin, L. Chen, J.-J. Yin, C.-C. Guo, Q.-Y. Chen, Eur. J. Org. Chem. (2005) 3994.
[19] C.H. Devillers, D. Lucas, A.K.D. Dime, Y. Rousselin, Y. Mugnier, Dalton Trans. 39 (2010) 2404.
[20] D.K. Dogutan, M. Ptaszek, J.S. Lindsey, J. Org. Chem. 72 (2007) 5008.
[21] K.M. Kadish, E.V. Caemelbecke, G. Royal, Electrochemistry of metalloporphyrins in nonaqueous media, in: K.M. Kadish, K.M. Smith, R. Guilard (Eds.), The Porphyrin Handbook, vol. 8, Academic Press, 2000, pp. 1–114, (Chapter 55).
[22] F.J. Kampas, K. Yamashita, J. Fajer, Nature 284 (1980) 40.
[23] K. Yamashita, Chem. Lett. (1982) 1985.
[24] M.A. Vorotyntsev, M. Casalta, E. Pousson, L. Roullier, G. Boni, C. Moise, Electrochim. Acta 46 (2001) 4017.
[25] M.A. Vorotyntsev, D.V. Konev, C.H. Devillers, I. Bezverkhyy, O. Heintz, Electrochim. Acta., in preparation. Q2
[26] V. Tsakova, S. Winkels, J.W. Schultze, Electrochim. Acta 46 (2000) 759.
[27] V. Tsakova, Personal communication.
[28] M.A. Vorotyntsev, V.A. Zinovyeva, D.V. Konev, Mechanisms of electropolymerization1redox activity: fundamental aspects, in: S. Cosnier, A.A. Karyakin (Eds.), Electropolymerization: Concepts, Materials and Applications, Wiley–VCH, Q3 Weinheim, 2010, pp. 27–50, (Chapter 2).
[29] C.H. Devillers, A.K.D. Dime, D. Lucas, H. Cattey, in press.
[30] A.F. Diaz, J.I. Castillo, J.A. Logan, W.Y. Lee, J. Electroanal. Chem. 129 (1981) 115.
[31] A.F. Diaz, J. Castello, K.K. Kanazawa, J.A. Loga, M. Salmon, O.F. Ajardo, J. Electroanal. Chem. 133 (1982) 233.
[32] A.A. Jarzecki, P.M. Kozlowski, P. Pulay, B.-H. Ye, X.-Y. Li, Spectrochim. Acta A 53 (1997) 1195.
[33] P.M. Kozlowski, A.A. Jarzecki, P. Pulay, J. Phys. Chem. 100 (1996) 7007. Q4
[34] L.J. Boucher, J.J. Katz, J. Am. Chem. Soc. 89 (1967) 1340.
[35] O.D. Ziganshina, M.D. Elkin, V.V. Nechaev, K.V. Berezin, J. Appl. Spectrosc. 71 (2004) 635.

[36] B. Minaev, H. Agren, Chem. Phys. 315 (2005) 215.
[37] S. Muralidharan, R.G. Hayes, J. Am. Chem. Soc. 102 (1980) 5106.
[38] G. Beamson, D. Briggs, High Resolution XPS of Organic Polymers: The Scienta ESCA300 Database, 1992.
[39] D.H. Karweik, N. Winograd, Inorg. Chem. 15 (1976) 2336.
[40] W.J. Landis, J.R. Martin, J. Vac. Sci. Technol. A 2 (1984) 1108.
[41] V.K. Kaushik, J. Electron Spectrosc. 56 (1991) 273.
[42] M. Kasha, H.L. Rawls, M.A. El-Bayoumi, Pure Appl. Chem. 11 (1965) 371.
[43] P.J. Spellane, M. Gouterman, A. Antipas, S. Kim, Y.C. Liu, Inorg. Chem. 19 (1980) 386.
[44] T. Ogawa, Y. Nishimoto, N. Yoshida, N. Ono, A. Osuka, Angew. Chem. Int. Ed. 38 (1999) 176.
[45] J.-H. Fuhrhop, in: D. Dolphin (Ed.), The Porphyrins, vol. 2, Academic Press, New York, 1978, p. 131.
[46] R.H. Felton, D. Dolphin, D.C. Borg, J. Fajer, J. Am. Chem. Soc. 91 (1969) 196.
[47] J. Fajer, D.C. Borg, A. Forman, D. Dolphin, R.H. Felton, J. Am. Chem. Soc. 92 (1970) 3451.
[48] J.-H. Fuhrhop, D. Mauzerall, J. Am. Chem. Soc. 91 (1969) 4174.
[49] T. Ogawa, Y. Nishimoto, N. Yoshida, N. Ono, A. Osuka, Chem. Commun. (1998) 337.

Please cite this article in press as: M.A. Vorotyntsev, et al., Magnesium(II) polyporphine: The first electron-conducting polymer with directly linked unsubstituted porphyrin units obtained by electrooxidation at a very low potential, Electrochim. Acta (2010), doi:10.1016/j.electacta.2010.06.001